Contents lists available at ScienceDirect

Arabian Journal of Chemistry

journal homepage: www.ksu.edu.sa

A highly selective nickel-aluminum layered double hydroxide nanostructures based electrochemical sensor for detection of pentachlorophenol

Mir Mehran Khan [a], Huma Shaikh [a], Abdullah Al Souwaileh [b,*], Muhammad Yar Khan [c], Madeeha Batool [d], Saima Q. Memon [e], Amber R. Solangi [a,*]

[a] National Centre of Excellence in Analytical Chemistry, University of Sindh, Jamshoro 76080, Sindh, Pakistan
[b] Department of Chemistry, College of Science, King Saud University, Riyadh 11451, Saudi Arabia
[c] School of Materials Science and Engineering, Zhejiang University, Hangzhou 310027, PR China
[d] Centre for Analytical Chemistry, School of Chemistry, University of the Punjab, Lahore 54590, Pakistan
[e] M.A Kazi Institute of Chemistry University of Sindh, 76080 Jamshoro, Sindh, Pakistan

ARTICLE INFO

Keywords:
Ni-Al-LDH nanostructures
Pentachlorophenol
Water samples
Electrochemical sensor
Ni-Al-LDH@GCE

ABSTRACT

With the widespread use of pesticides, environmental pollution has elevated to a top priority for humans. The pentachlorophenol (PCP) is one of the most dangerous chlorophenols, employed as pesticides, fungicides, and wood preservatives. In the current study, a nickel-aluminum layered double hydroxide modified glassy carbon electrode (Ni-Al-LDH@GCE) was used to build a straight forward, environmentally friendly, and accurate electrochemical sensor for the measurement of PCP. The fabricated Ni-Al-LDH was principally assessed using a variety of characterization methods to confirm its functionalities, morphology, porosity and crytallanity. The proposed Ni-Al-LDH@GCE sensor was also characterized electrochemically for the evaluation of its conductivity using electrochemical impedance spectroscopy (EIS) and cyclic voltammetry (CV). The linear dynamic range of the developed ultra-sensitive Ni-Al-LDH@GCE based electrochemical method was found as 0.05 to 50 μM at a scan rate of 50 mV/s in Britton-Robinson buffer of pH 6 for PCP. The limit of detection (LOD) and limit of quanitification (LOQ) of electrochemical sensor for PCP were determined as 0.004 μM and 0.0132 μM, respectively. The sensor's analytical suitability was evaluated using real water samples that showed the acceptable recovery values.

1. Introduction

Pentachlorophenol (PCP) is a synthetic chemical that is classified as an organochlorine compound (Taqvi et al., 2022, Meskher et al., 2023). When chlorine is added to phenols, a substantial class of extremely harmful environmental contaminants known as chlorophenols is created. The quantity of chlorine atoms in the molecule or structure of chlorophenols was found to affect their toxicity (Wang et al., 2020). PCP, one of the most dangerous chlorophenols, is used in a variety of industrial and agricultural processes as a disinfectant, bactericide, Algaecide, fungicide and preservative for wood (Meskher et al., 2023). Due to its sufficient solubility in water such as 0.020 g/L; PCP is detected in surface waters and sediments, rainwater, drinking water, aquatic organisms, soil, and food, as well as in human milk, adipose tissue, and urine (Lee et al., 2006). Because of its high toxicity, extended persistence and resistance to degradation, PCP can lead to negative effects such as acute toxicity, mutagenicity, and carcinogenicity (Wang et al., 2020, Mustafa, 2023a,b). The United States Environmental Protection Agency (US EPA) has classified PCP as a priority pollutant. According to their guidelines, the maximum allowable concentration of PCP in drinking water has been set at 1 μg/L (Feng et al., 2015). Thus, the need for a quick, easy, and accurate approach to detect PCP at a trace level in various environmental samples became critical. For the detection of PCP, a variety of techniques have been used during the last few decades, including HPLC (Ammeri et al., 2015), gas chromatography (Zhao, 2014) GC–MS (Zhou et al., 2007), TLC (Kang et al., 2010) and electrochemical analysis (Yang et al., 2022). The electrochemical sensors have garnered the most interest among the technologies mentioned above due

* Corresponding authors.
E-mail addresses: aswieleh@hotmail.com (A. Al Souwaileh), ambersolangi@gmail.com (A.R. Solangi).

https://doi.org/10.1016/j.arabjc.2024.105604
Received 25 July 2023; Accepted 2 January 2024
Available online 3 January 2024

to their ease of use, high sensitivity, quick analysis, and affordability (Salmanpour et al., 2017, Alizadeh et al., 2021, Mehmandoust et al., 2021). The ability to be sensitive and selective in real matrix, cost effectiveness, and operational simplicity are the major factors to take into account when integrating any sensor platform. Because of their simplicity, low cost, sensitivity, and ability to be selective over more complex instruments, electrochemical sensors have potential to be used in this area (Baig and Kawde, 2015, Jin and Maduraiveeran, 2017, Mustafa, 2023a,b). To enhance the electro catalytic activity and selectivity of bare electrodes for the detection of environmental contaminants, various compounds have been utilized as modifiers (Sajid et al., 2016). However, due to their remarkable qualities, distinctive performance, and vast variety, nanomaterials have attracted a lot of attention as electrochemical sensing materials. The widespread use of nanoparticles in electrochemical sensing and their numerous applications are related to their extraordinary mechanical, chemical, physical, and electrical properties, which include a vast surface area (Maduraiveeran and Jin, 2017). In addition to offering a large number of active sites for the required electrochemical reactivity, the large surface area is crucial for enhancing the kinetics of electrochemical reactions (Baig and Kawde, 2016). Furthermore, nanomaterials can be further functionalized with appropriate chemical moieties to increase the selectivity towards particular analytes. The layered double hydroxides (LDH) have been used recently for several applications. LDH have been widely employed in many fields, such as photochemistry, adsorption, CO_2 capture, medication delivery, and as retardant additives; however, the scope of their use as well as their overall performance are severely constrained by the inevitable accumulation of the lamellar LDH Flakes (Jiménez-López et al., 2021). In the previous ten years, the synthesis of two-dimensional (2D) nano sheets of layered solids, such as metal chalcogenides (Liang et al., 2015) metal phosphates and phosphonates (Wang and O'Hare, 2012), layered metal oxides (Mallakpour et al., 2021) as well as layered double hydroxide (Wang and O'Hare, 2012, Bukhtiyarova, 2019) have gotten a lot of attention. The 2D nano sheets, which have a lateral size range from sub micrometric to several tens of micrometers and a thickness of about one nanometer, have a higher specific surface area and more active sites. They can be used for both fundamental research and as a building block to create a variety of functional materials (Kikhtyanin et al., 2018). LDHs are two-dimensional nanostructured materials with unique physicochemical properties. They belong to the fascinating class of inorganic materials that can have tunable chemical and structural composition. They are also known as hydrocalcite or anionic clays. They are composed of layers of positively charged metal hydroxides that are separated from one another by a few water molecules and charge-neutralizing anions. The typical formula for them is $[M_{2+1-x}M_{3+x}(OH)_2]_{x+}(An)_{x/n}{\cdot}mH_2O$, where M^{2+} and M^{3+} are divalent and trivalent metal cations, respectively, and An is the interlayer guest ion with n-valence. The range of x's values is 0.22 to 0.33 (Auerbach et al., 2004). LDHs are frequently prepared using co-precipitation, ion exchange, electrochemical synthesis, hydrothermal synthesis, calcination recovery, etc. (Tonelli et al., 2013, Yu et al., 2017). The synthesis method should be simple, cost-effective, efficient, prolific, and capable of producing nanostructures that are environmentally friendly (Saratale et al., 2018). The co-precipitation method is one of the simple, cost-effective and swift one-pot synthesis strategies that can produce efficient LDHs. In a typical co-precipitation technique, an aqueous solution of metal (II) cation and metal (III) cation is normally used in an adequate ratio, and the solution containing the target anion that needs to be intercalated is slowly added to the aqueous solution (Jijoe et al., 2021). In this study, we aimed to fabricate a sensitive and robust electrochemical sensor based on Ni-Al-LDH for the selective detection of PCP. Ni-Al-LDH was effectively synthesized using a co-precipitation procedure. The synthesized Ni-Al-LDH was used to modify the GCE surface, and after optimizing various parameters, a highly sensitive and specific sensor for the detection of PCP was produced. Because of Ni-Al-LDH's exceptional catalytic activity, extensive surface area, and high conductivity, the produced sensor demonstrated excellent sensitivity and selectivity towards a variety of PCPs.

2. Experimental work

2.1. Chemical and reagents

The chemicals of high purity were utilized for this work, which were obtained from reputable suppliers such as Sigma Aldrich and Merck. The chemicals employed included nickel nitrate hexahydrate, from Sigma Aldrich (Indonesia) aluminum nitrate nonahydrate, from Sigma Aldrich (Indonesia), sodium hydroxide, from Merck (China) pentachlorophenol from Sigma Aldrich (Indonesia), phenol, 2,4,6-trichlorophenol, cadmium chloride, mercury(II) sulfate, iron nitrate, borate buffer, phosphate buffer, hydrochloric acid, zinc acetate, and lead acetate from Merck (China). These chemicals were used in their as-purchased state without undergoing additional purification. Deionized water was utilized throughout the entire experimental procedure.

2.2. Instrumentation

Several characterization techniques, including scanning electron microscopy (SEM), Fourier transform infrared spectroscopy (FTIR), X-ray diffraction XRD and Brannauer Emmet Teller (BET) were employed to characterize the synthesized Ni-Al-LDH nanostructures. In order to examine the morphology of synthesized material, SEM was used. For examining the crystalline nature of produced nanostructures, powder X-ray Diffractometer (XRD-7000-Shimadzu scientific-instrument) was utilized, and the specific surface area and pore size distribution of the nanostructured material were determined using the BET (Quanta chrome-instrument) technique. To verify the various functionalities of the produced material, FTIR (Themo Nicolet-5700) was employed. The electrochemical measurement of PCP was conducted using an electrochemical workstation (AutoLab CHI-760-USA) equipped with a three-electrode setup.

2.3. Synthesis of nickel aluminum LDH by co-precipitation method

To synthesize nickel aluminum nitrate LDH, a method of Meskher et al. (2023) was used with slight modification. Precisely, a solution was prepared by dissolving 0.2 M of nickel nitrate hexahydrate $Ni(NO_3)_2{\cdot}6H_2O$ and 0.1 M of aluminum nitrate nonahydrate $Al(NO_3)_3{\cdot}9H_2O$ in 100 mL of deionized water. The solution was thoroughly mixed to ensure complete dissolution of the salts. Subsequently, a 1 M solution of sodium hydroxide (NaOH) was added drop wise to the solution under continuous stirring. The NaOH served as the source of hydroxide ions (OH^-) necessary for the reaction. Throughout the process, the pH of the solution was carefully maintained at 9. The solution was then allowed to stand for 24 h, enabling the formation of precipitates. After the aging period, the resulting precipitates were separated from the liquid by filtration. The collected precipitates were further dried at 80 °C for 2 h to remove any remaining moisture. Finally, the dried precipitates were stored for future use in subsequent experiments or other applications.

2.4. Procedure for electrode modification

The glassy carbon electrode (GCE) was modified with Ni-Al-LDH using a drop-casting technique as described in the literature (Kumar et al., 2020). Precisely, 10 mg of Ni-Al-LDH was added to 2.5 mL of deionized water. Additionally, 20 µL of a 5 % Nafion solution, serving as a binder, was included in the water. The resulting solution was thoroughly mixed and homogenized using sonication for a duration of 30 min. Before the modification process, the surface of the electrode was polished using 0.5 µm pore size of alumina powder and then rinsed with deionized water. Subsequently, the prepared Ni-Al-LDH solution was

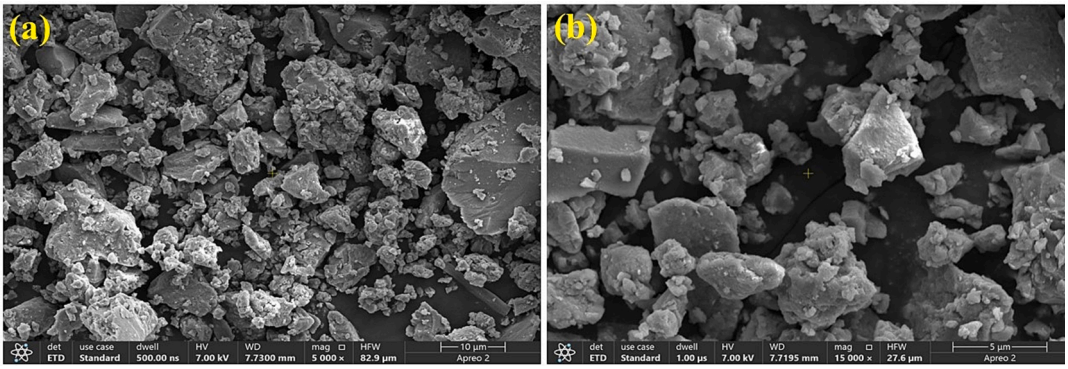

Fig. 1. SEM images of Ni-Al-LDH nanostructures (a) with low resolution and (b) with high resolution.

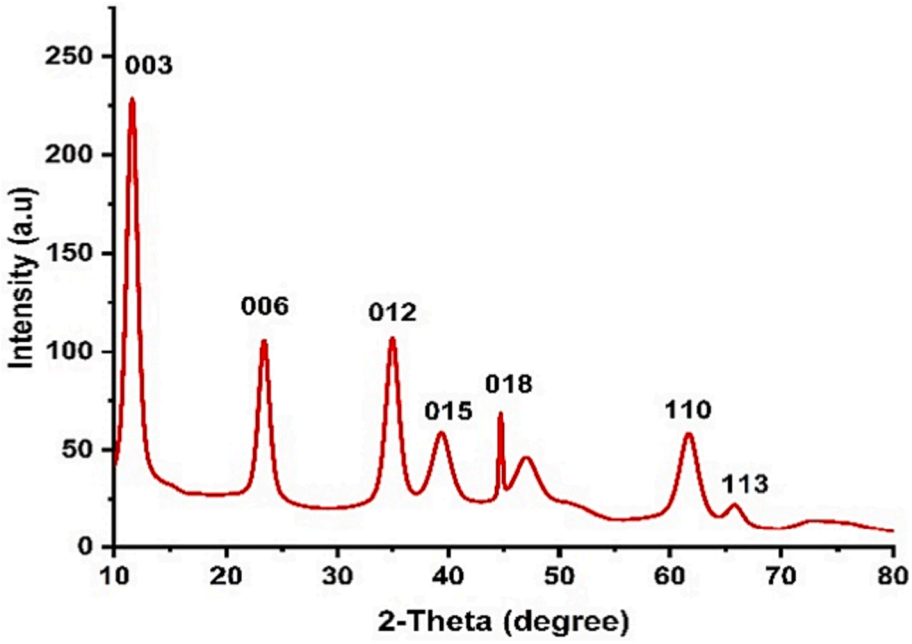

Fig. 2. XRD pattern of Ni-Al-LDH nanostructures.

applied to the electrode surface by dropping 5 µL of the solution onto it. Finally, the modified electrode was left to dry at room temperature, allowing the solvent to evaporate and leaving the Ni-Al-LDH coating on the electrode surface (Khand et al., 2021).

2.5. Real sample collection and preparation

To determine the maximum concentration of PCP in water samples, four different sources were used: the Khipro canal in the town of Khipro, Sindh, Pakistan, the River Indus water at Jamshoro, Sindh, Pakistan, the industrial wastewater at Kotri Industrial Area, Kotri, Sindh, Pakistan and the National Centre of Excellence in Analytical Chemistry (NCEAC) at the University of Sindh, Jamshoro, Pakistan. For the synthetic sample, a real water sample from NCEAC was taken and subjected to filtration using a 0.3 µm pore-sized filter paper. Subsequently, 2 mL of a 1 mM PCP solution and interfering species were added in a 1:1 ratio. The resulting solution was then diluted to a total volume of 500 mL. The samples from Khipro canal water, River Indus water and industrial wastewater were collected and taken to the laboratory and filtered using a filter paper with a 0.3 µm pore size filter paper. Subsequently, the water samples were diluted to a concentration of 0.1 M using the Britain Robinson buffer in a ratio of 2:10 v/v. The standard addition method was employed to assess the accuracy of PCP in the real water samples. This involved spiking the samples with a standard concentration of PCP.

3. Results and discussion

3.1. Characterization

In order to analyze the surface morphology of the nanostructures, SEM was employed. Fig. 1 shows SEM images of Ni-Al-LDH. It can be observed that Ni-Al-LDH display a flat and smooth surface with clear evidence of non-rigid shapes caused by the presence of nano-structural strains.

To investigate the phase structure and crystalline nature of the synthesized Ni-Al-LDH, XRD analysis was conducted. The XRD pattern in Fig. 2 exhibits distinct reflections corresponding to specific crystal planes of a crystalline LDH, including (003), (006), (012), (015), and (018). Additionally, two other patterns corresponding to (110) and (113) planes of LDH were observed within the 2-theta range of 62-66 degrees. These findings confirmed that the Ni-Al (NO_3^-) LDH primarily displays reflections characteristic of hydrocalcite like LDH (JCPDS 33-0426), with no indication of other crystalline phases. These results are consistent with previous research (Abdolmohammad-Zadeh et al., 2013). The crystal size of the nanostructures was estimated to be 30 nm using the Debye-Scherer equation.

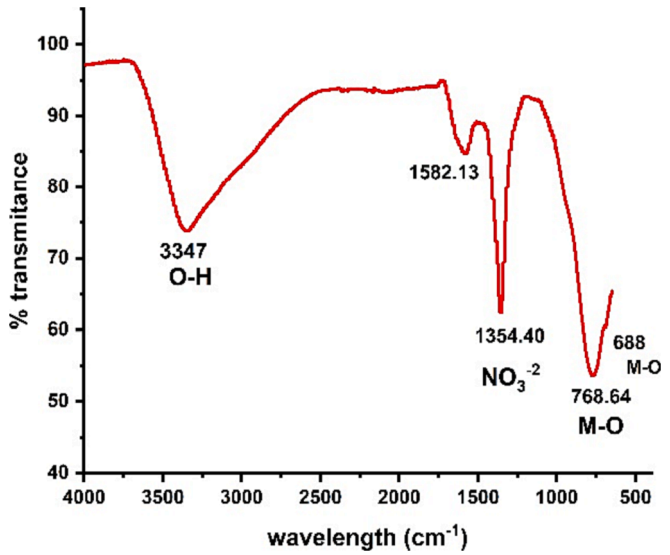

Fig. 3. FTIR spectrum of Ni-Al-LDH.

FTIR was employed to validate the chemical composition of the prepared Ni-Al-LDH precipitates (Fig. 3). The broad band observed around 3347 cm^{-1} is attributed to the –OH stretching mode of intermolecular hydrogen bonding between the hydroxyl groups of the LDH layers and the interlayer water molecules. Weak bands at 1582 cm^{-1} indicated the bending mode vibration of the OH functional group. As the LDH contains nitrate anions, vibration peaks corresponding to NO_3^- groups were observed around 1354 cm^{-1}. However, no bands associated with CO_3^{2-} anions were detected, indicating the absence of CO_2 contamination. The peaks appearing below 1000 cm^{-1} can be attributed to the vibrations of metal–oxygen (M-O, M-O-M, O-M-O) bonds within the LDH layers. This observation is attributed to the selective dissolution of divalent cations and preferential precipitation of trivalent cations as hydroxides, due to the higher acidity and lower solubility of trivalent cation hydroxides.

Furthermore, N_2 sorption data revealed high surface area and pore volume of the produced Ni-Al-LDH. Fig. 4(a) indicated type V/H2 and V/H3 N_2 adsorption–desorption isotherms with hysteresis loops indicative to mesoporous structure and ink bottled porous shaped pores, respectively. MBET analysis revealed (Fig. 4b) that the specific surface area of the Ni-Al-LDH was determined to be 22.34 m^2/g, which aligns with the expected composition ratio of LDH particles and confirms its porous structure. The pore volume was measured as 0.104 cc/g, (Fig. 4c) and the pore diameter was found to be 3.12 nm, indicating the presence of a mesoporous structures in the Ni-Al-LDH.

3.2. *Electrochemical characterization of (Ni-Al-LDH) modified GCE*

Cyclic voltammetry and electrochemical impedance spectroscopy (EIS) studies were conducted to investigate the electrochemical behavior and conductivity of Ni-Al-LDH modified glassy carbon electrode (Ni-Al LDH@GCE) and bare glassy carbon electrode (bare GCE). These studies were performed using 0.1 M KCl as the electrolyte solution and solutions containing a redox probe consisting of 5 mM $K_3Fe(CN)_6$ and $K_4Fe(CN)_6$. Fig. 5(a) displays the interfacial characteristics of the bare and modified glassy carbon electrodes through EIS. The EIS study measures the charge transfer resistance (Rct) for any analyte present in the electrochemical system. The impedance spectra, depicted as a Nyquist plot, illustrates the Rct which depends on the electron transfer kinetics of the redox probe at the electrode surface. The diameter of the semicircle curve in the Nyquist plot is used to determine Rct. In general, a broader semicircle curve indicates higher resistance, while a narrower semicircle curve suggests lower resistance. The Nyquist plot of the bare GCE showed a broader semicircle curve, indicating high resistance, whereas the Nyquist plot of the Ni-Al-LDH@GCE exhibited a narrower semicircle curve, indicating lower resistance. This EIS study clearly suggests that Ni-Al-LDH@GCE is highly effective in facilitating

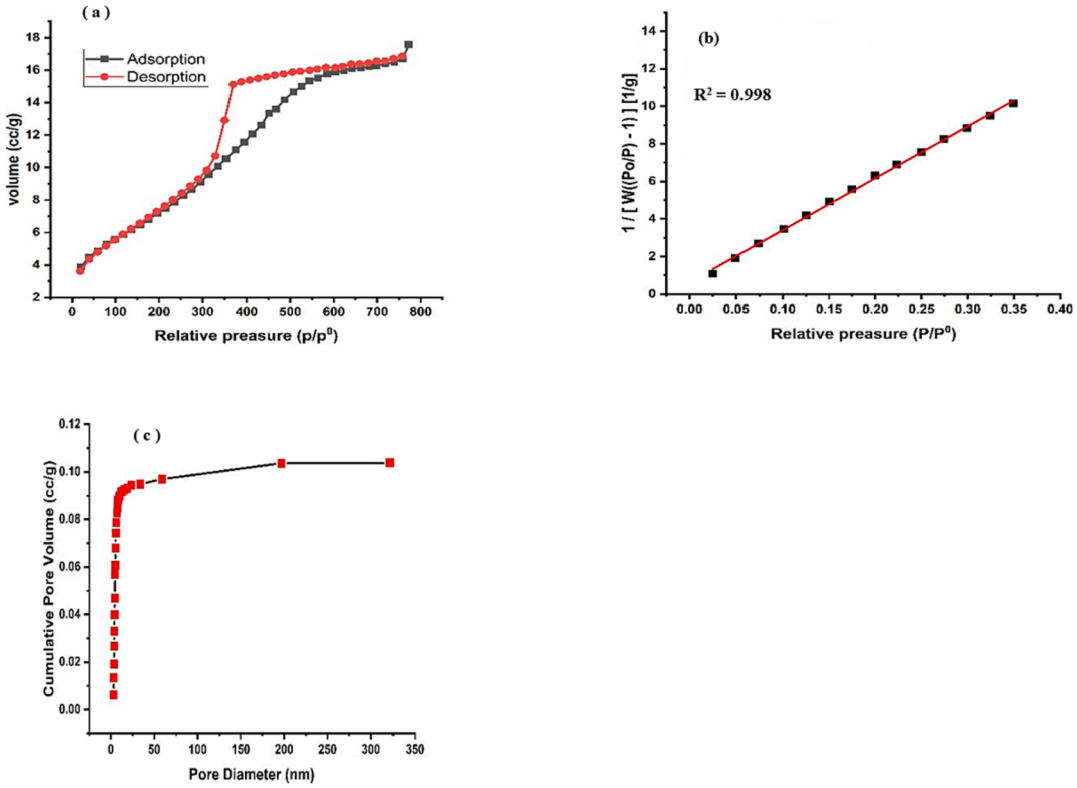

Fig. 4. (a) BET Adsorption-desorption Isotherm (b) multiple point of BET plot (c) BJH pore volume graph of Ni-Al-LDH.

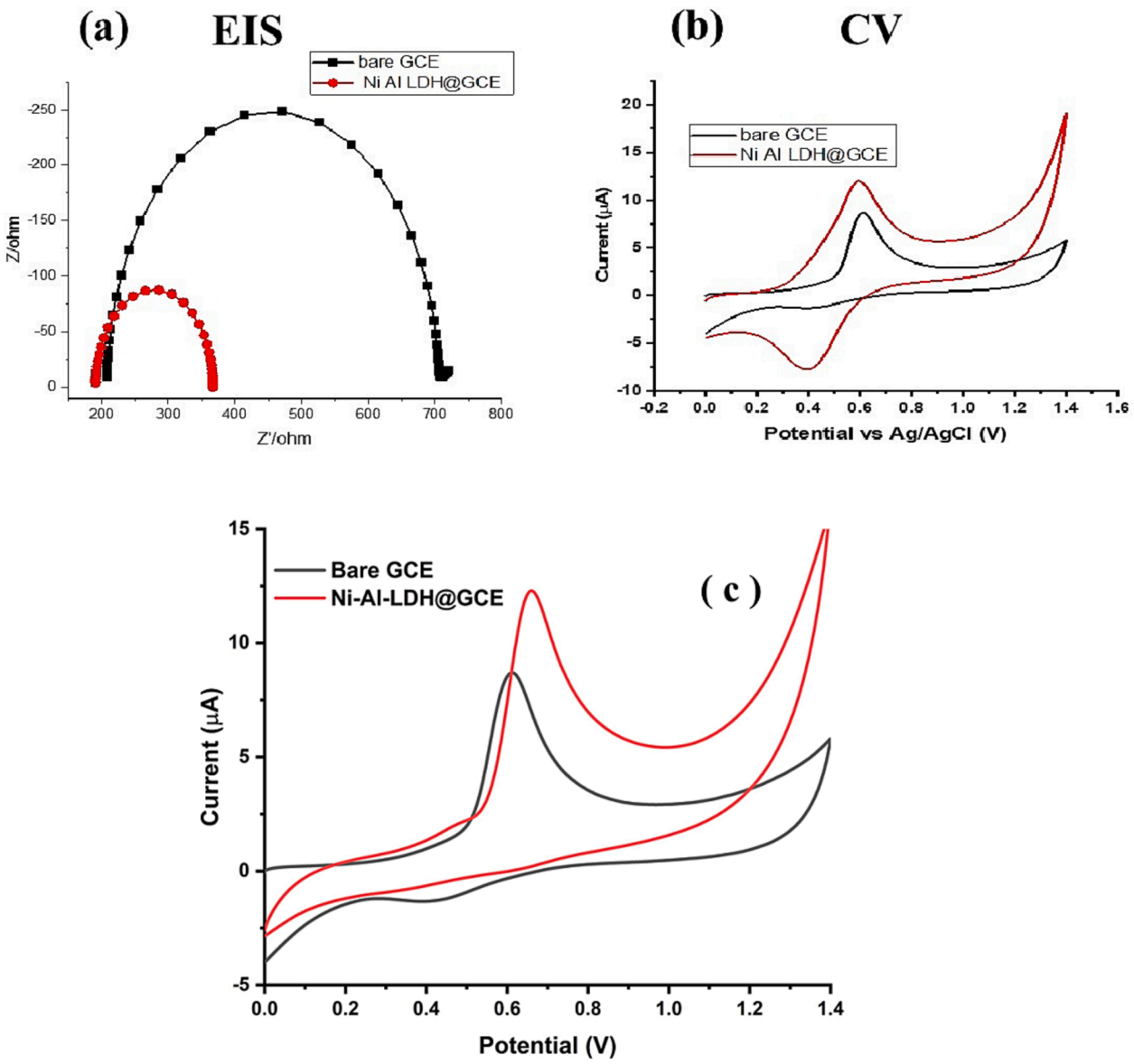

Fig. 5. (a) EIS Nyquist plot of Ni-Al-LDH@GCE and bare GCE, (b) CVs redox peak current response of Ni-Al-LDH@GCE and bare GCE at 50 mV/s (c) CV's response of 5 μM of PCP using Ni-Al-LDH@GCE and bare GCE in the presence of BR buffer of pH 6.

electrochemical determinations, as it provides the lowest resistance. The cyclic voltammetric anodic peak current (Ipa) response of the bare and modified GCE was recorded, as shown in Fig. 5(b). Both the Ni-Al-LDH@GCE and the bare GCE exhibited redox behavior in the electrolyte solution. However, the Ni-Al-LDH@GCE showed a significantly greater redox peak current response compared to the bare electrode. This good electrochemical performance of Ni-Al-LDH@GCE can be attributed to the excellent electronic conductivity of the synthesized Ni-Al-LDH and the affinity reaction on the engineered-interface-based hydroxyl groups in Ni-Al-LDH which is likely to have high interaction with PCP. This observation indicates that Ni-Al-LDH is an excellent candidate for electrochemical detection of numerous analytes. Based on its cyclic voltammetry redox behavior, it can be concluded that Ni-Al-LDH is a highly promising material for electrochemical sensing applications. Fig. 5c shows the comparison of CV curves of 5 μM of PCP at Ni-Al-LDH@GCE and bare GCE. The results reveal that Ni-Al-LDH@GCE produced higher current values as compared to bare GCE. These results confirmed that Ni-Al-LDH@GCE is more sensitive towards PCP as compared to bare GCE.

3.3. *The effect of supporting electrolytes*

In order to investigate the impact of different electrolytes on the current response in cyclic voltammetry, we conducted a study to understand the role of supporting electrolytes in facilitating charge transfer. Four different supporting electrolytes with varying pH values were utilized: 0.1 M phosphate buffer (pH 7.4), 0.1 M NaOH (pH 12), 0.1 M borate buffer (pH 8.1), and Britton–Robinson buffer (pH 4). The purpose of this electrolyte study was to explore the influence of electrolyte on the current response. The electrolytes at their most relevant pH were used. Starting from a neutral pH, we systematically increased the pH to a highly basic level of approximately 12. The obtained results, as shown in Fig. 6, demonstrated that the maximum current response was achieved using 1 μM PCP in 0.1 M Britton Robinson buffer at pH 4. Based on this finding, we concluded that Britton Robinson buffer would be the most suitable supporting electrolyte for further measurements and analyses. By conducting this buffer study, we gained valuable insights into the optimal conditions for achieving the maximum current response in cyclic voltammetry experiments. The selection of Britton Robinson buffer as the supporting electrolyte was based on its ability to provide the

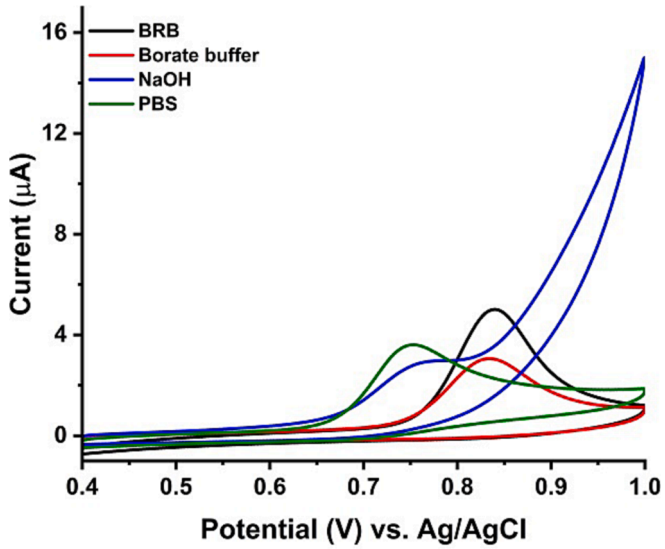

Fig. 6. CV's response of PCP using Ni-Al-LDH@GCE in the presence of different supporting electrolytes.

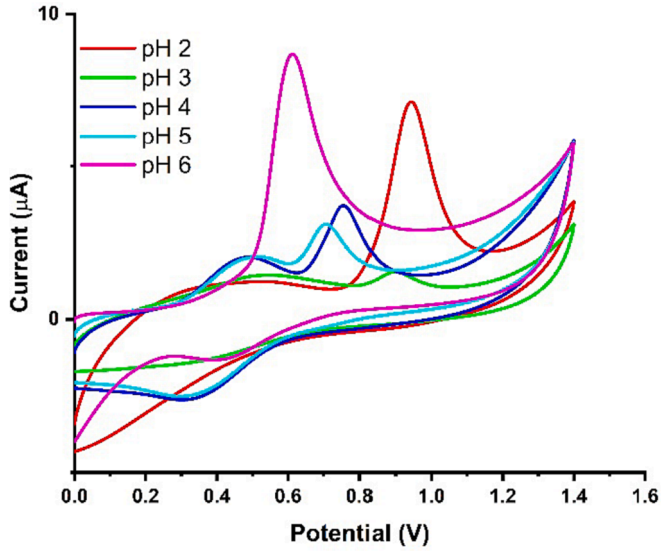

Fig. 7. CV Ipa response of 5 μM PCP using Ni-Al-LDH@GCE at different pH of BRB at scan rate 50 mV/s.

highest current response for the specific analyte of interest i-e PCP.

3.4. Investigation of pH of supporting electrolyte

In order to determine the highest anodic peak current response of Ni-Al-LDH@GCE for 5 μM PCP, experiments were conducted to optimize the most suitable pH of Britton-Robinson Buffer. The pH values were varied in the range of 2 to 6. The experiments were performed with a scan rate of 50 mV/s. The results, shown in Fig. 7, illustrated the Ipa response of PCP in BRB supporting electrolyte at pH values ranging from 2 to 6. The pH study revealed that the maximum Ipa response occurred at pH 6. This discovery indicated that pH 6 was the most favorable pH of BRB for detecting and analyzing PCP using the Ni-Al-LDH@GCE. However, we observed lower Ipa responses of PCP at acidic pH of BRB. These results reveal that the Ni-Al-LDG@GCE is capable to facilitate proton removal of PCP at pH 6 of BR buffer. Additionally, the modified sensor exhibited excellent stability at pH 6, further supporting the choice of pH 6 for optimizing other parameters to ensure accurate determination of

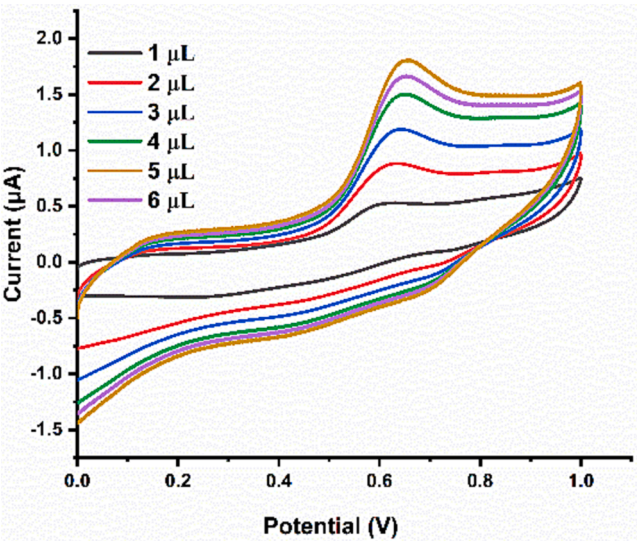

Fig. 8. CV Ipa response of 1 μM PCP using different amounts of Ni-Al-LDH on Ni-Al-LDH@GCE BRB of pH 6 and scan rate of 50 mV/s.

PCP.

3.5. Effect of amount of Ni-Al-LDH on Ni-Al-LDH@GCE for determination of PCP

The amount of Ni-Al-LDG was optimized in the range of 1 to 6 μL. The Ipa response of PCP kept increasing from deposition of 1 μL to 5 μL as expected because more amount of Ni-Al-LDH facilitated swift redox reaction of PCP at Ni-Al-LDH@GCE. However, further increase in the amount of Ni-Al-LDH decreased the Ipa response of PCP may be due to the decreased surface area of the electrode (Fig. 8).

3.6. Effect of scan rate

To verify the diffusion control response of Ni-Al LDH@GCE, an analysis of the kinetics at various scan rates was conducted. Fig. 9 presents the cyclic voltammogram of a 1 μM PCP at different scan rates. The oxidation process of PCP on the Ni-Al-LDH@GCE was investigated. The results revealed that by increasing the scan rates, a distinct increase in anodic peak current response was facilitated by Ni-Al-LDH@GCE. When examining the response of the sensor in a 1 μM PCP solution at different scan rates, we observed a linear correlation between the peak current and the scan rate, indicating that the behavior of the modified electrode was diffusion-controlled. Fig. 9(b) illustrates the relationship between the square root of scan rates $mV/s^{1/2}$ and the anodic peak current, with an R^2 value of 0.9846, confirming the diffusion-controlled nature of the LDH@GCE.

3.7. Linear calibration study

The list of analytical Figure of merits of the developed electrochemical method is given in Table 1. The calibration curve for PCP detection is presented in Fig. 10, demonstrating a linear correlation between the peak current and PCP concentration within the range of 0.05–50 μM. The linear response exhibited an R^2 value of 0.992, indicating favorable analytical behavior of Ni-Al-LDH@GCE within this linear range. Fig. 10(a) illustrates the differential pulse voltammetry (DPV) at different concentrations of PCP and its corresponding linear peak current response. To determine the sensitivity of the proposed sensor for detecting PCP, we calculated the limit of detection (LOD) and limit of quantification (LOQ). The LOD was found as 3.3 times the standard deviation of the blank solution divided by the slope of the

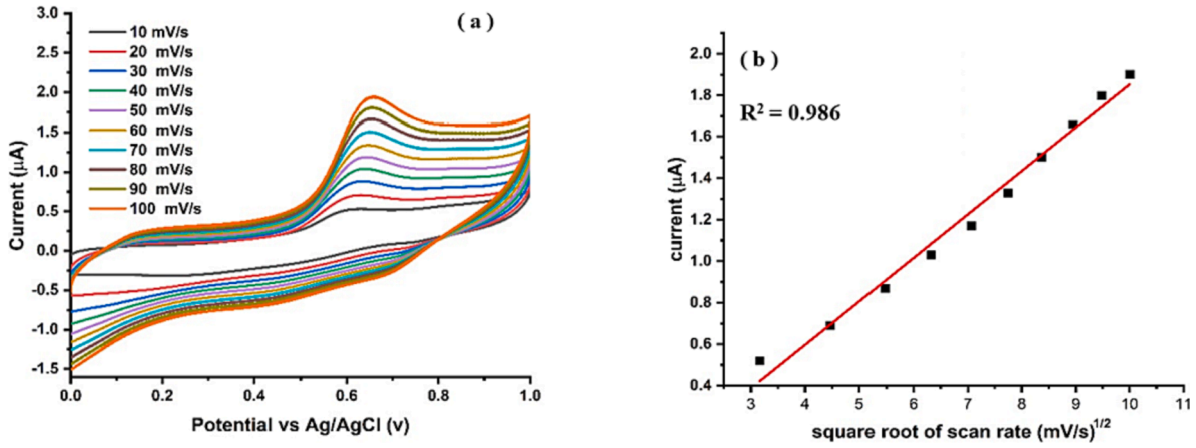

Fig. 9. (a) Effect of scan rate on Ipa response Ni-Al-LDH@GCE in 1 μM PCP using BRB pH 6, (b) Plot of square root of scan rate v/s Ipa.

Table 1
List of analytical figures of merit of the developed electrochemical method for the quantitative detection of PCP.

Sr. No.	List of Analytical Figures	Values
1	LOD	0.004 μM
2	LOQ	0.0132 μM
3	Linear Range	0.05–50 μM
4	R^2 (linearity)	0.992
5	Slope (a)	$2.08x10^{-7}$
6	Intercept (b)	3.7×10^{-6}
7	**Intraday precision**	
a)	0.05 μM (n = 05)	0.24 %
b)	25 μM (n = 05)	0.32 %
c)	50 μM (n = 05)	0.24 %
8	**Interday precision**	
a)	0.05 μM (n = 100)	2.45 %
b)	25 μM (n = 100)	1.95 %
c)	50 μM (n = 100)	1.75 %

calibration curve. Similarly, the LOQ was determined as 10 times the standard deviation of the blank solution divided by the slope of the calibration curve (Amin et al., 2019). The LOD and LOQ values were found to be 0.004 μM and 0.0132 μM, respectively. In order to evaluate the reproducibility and precision of fabricated Ni-Al-LDH@GCE, the intraday and interday precisions were calculated (Table 1). The results revealed that Ni-Al-LDH@GCE reproduces results with good precision in both inter- and intraday analysis. Hence, it can be reused several times and is capable of producing reliable results.

3.8. *Evaluation of stability of Ni-Al-LDH@GCE*

To evaluate the long-term measurements, the proposed Ni-Al-LDH@GCE was checked for its stability for around three weeks. Fig. 11 shows the stability curves of 1 μM of PCP for 25 different runs. The results showed %RSD less than 5 %. For long-term analysis of the PCP, the fabricated sensor should be stable. Thus, stability is the most important parameter in electrochemical measurements. The proposed sensor was also evaluated for its reproducibility by recording response of 0.05, 25 and 50 μM of PCP 5 times each day and for 20 consecutive days The obtained results revealed that the fabricated sensor was highly stable for up to 18 consecutive days with a calculated %RSD of less than 5 % (Table 1). Moreover, the RSD for the stability of the proposed sensor in between 18 and 20 days was recorded as 2.45 % which confirms the stable nature of Ni-Al-LDH@GCE (See Fig. 12).

3.9. *Effect of interfering ions*

To assess the selectivity of Ni-Al-LDH@GCE, experiments were carried involving various interfering species, including phenol, trichlorophenol, cadmium, nickel, iron, mercury, lead, and zinc, in the presence of 1 μM pentachlorophenol. The concentration of all the interfering compounds was also kept 1 μM. The results, depicted in Fig. 11, demonstrate that these interfering species had minimal impact on the detection of PCP. There was no significant change observed in the peak current response of the analyte (PCP). This outcome indicates that Ni-Al LDH@GCE exhibits a high level of selectivity for the detection of

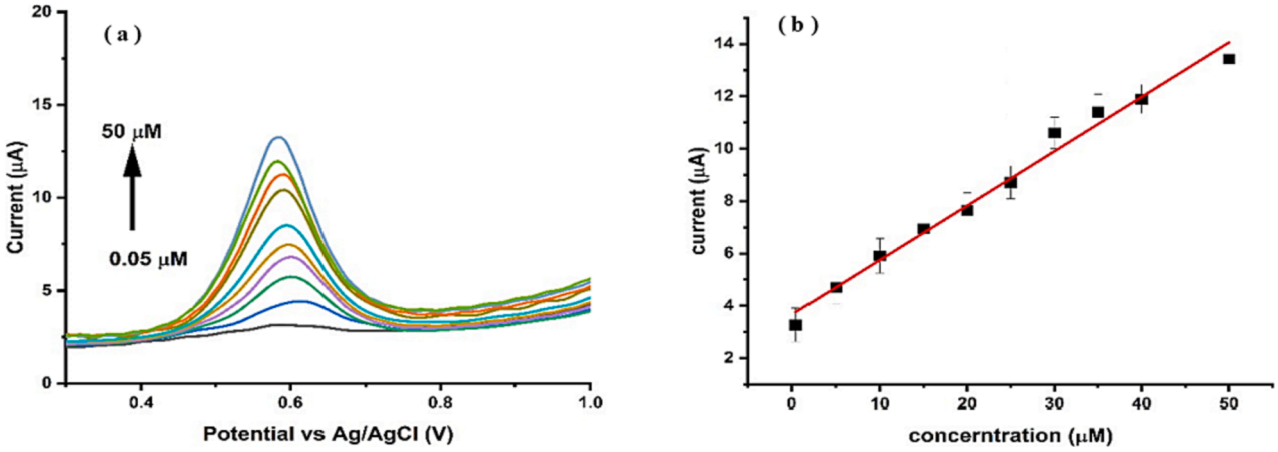

Fig. 10. (a) The DPV response of PCP at different concentration (0.05–50 μM) using Ni-Al-LDH@GCE at scan rate 50 mV/s in BRB of pH 6 (b) The plot of linear calibration curve for DPV response of PCP v/s concentration.

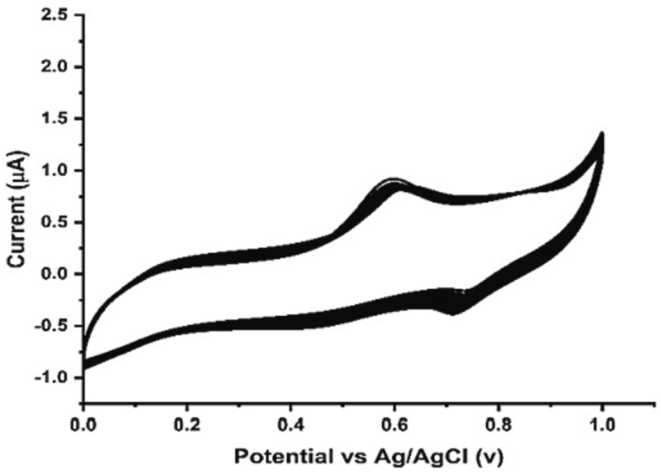

Fig. 11. Stability of proposed sensor for consecutive 25 repeated cycles.

PCP, making it well-suited for application in real sample analysis.

3.10. Analysis of real samples

To evaluate the accuracy of the PCP sensor in real samples, a recovery test was conducted using water samples collected from Khipro village, the National Centre of Excellence in Analytical Chemistry (synthetic water), Indus River at Jamshoro and Industrial wastewater at Kotri. The collected samples were filtered and diluted with BR buffer solution of pH 6, and then spiked with a known concentration of PCP. The response percentage of PCP was calculated and found to be in the range of 95–132 % (Table 2). This indicates the excellent sensitivity and suitability of the Ni-Al LDH@GCE sensor for detecting PCP in real samples. To ensure reproducibility, each test was performed three times and consistent peak current responses were recorded for all water samples. When comparing the electrochemical performance of various proposed sensors for PCP detection, it becomes evident that most of the reported sensors are either expensive or complex to use, making them impractical for underdeveloped countries. Additionally, some sensors with lower costs have demonstrated poor sensitivity in detecting PCP. In contrast, the proposed Ni-Al-LDH@GCE sensor stands out due to its high stability, affordability, and exceptional sensitivity towards PCP detection. These features distinguish it from other reported sensors shown in Table 3. It can be observed that Ni-Al-LDH@GCE sensor shows lowest limit of detection and broad linear range when compared with other electrochemical sensors for PCP (See Table 3).

4. Conclusion

In this study, the successful synthesis of Ni-Al-LDH nanostructure was achieved, and its characterization was conducted using advanced analytical techniques. The nanostructured material Ni-Al-LDH was then used to modify a glassy carbon electrode, creating an electrochemical sensor. This sensor exhibited outstanding performance for the detection of PCP, having a low detection limit of 0.004 μM and a linear dynamic range of 0.05–50 μM. Furthermore, the sensor demonstrated excellent stability, selectivity, and sensitivity under optimal conditions. To verify the accuracy of the sensor, real sample testing was performed. These results further confirmed the reliability and effectiveness of the sensor in real matrix. Overall, this research introduces a novel and promising approach for the efficient detection of PCP. The developed sensor has significant potential for applications in environmental monitoring and water quality assessment.

Declaration of competing interest

The authors declare that they have no known competing financial interests or personal relationships that could have appeared to influence

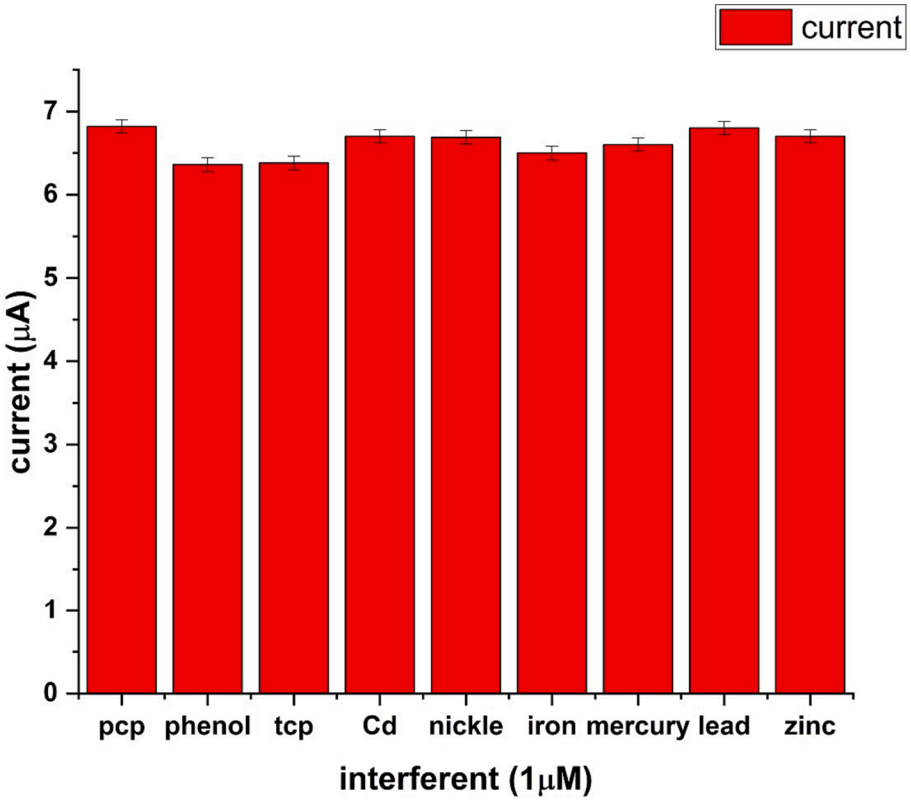

Fig. 12. Bar chart of interfering species.

Table 2
Real application of Ni-Al-LDH@GCE in water samples.

Samples	Spiked μM	Detected μM	RSD %	Recovery %
Synthetic water	0	14.8	4.3	0
	5	20	3.76	104
	10	29.9	3.57	99.5
	15	45.5	1.31	104
Khipro canal Water	0	0	0	0
	5	5.01	2.55	101
	10	14.7	1.49	97.5
	15	29.6	1.19	99
River Indus at Jamshoro	0	0	0	0
	5	4.92	1.54	98.4
	10	9.68	2.12	96.8
	15	14.76	1.01	98.4
Industrial Wastewater (Kotri)	0	2.5	2.23	0
	5	7.21	1.24	94.2
	10	12.45	1.75	99.5
	15	18.21	1.11	104.733

Table 3
Comparison of Ni-Al-LDH@GCE with reported sensor for detection of PCP.

Sensors	Technique	Linear range (μM)	LOD (μM)	References
CuS nanocomposite	DPV	1.88–76	0.6	(Zhao et al., 2013)
CeO_2–GR	DPV	5–150	0.5	(Yang et al., 2022)
(Al-MCF)	DPV	100–5000	80	(Ya et al., 2018)
(Pt-SiPy+Cl−).	DPV	1.37 to 21.4	1.10	(dos Santos et al., 2016)
TiO_2-CNTs	DPV	0.4–0.3	0.011	(Zhang et al., 2011)
LDH/HA	DPV	0.003–0.32	0.02	(Yuan et al., 2013)
NiCo-LDH/rGO-CuO	Cv	1–50	0.0126	(Zhang et al., 2021)
MWCNT-EP	SWVs	0.2–12	0.006	(Remes et al., 2012)
NiCo-LDH/rGO-CuO	Cv	1–50	0.01264	(Meskher et al., 2023)
Ni-Al-LDH	DPV	0.05–50	0.004	Present work

the work reported in this paper.

Acknowledgment

This project was supported by Researchers Supporting Project number (RSP2024R238), King Saud University, Riyadh, Saudi Arabia.

References

Abdolmohammad-Zadeh, H., Jouyban, A., Amini, R., et al., 2013. Nickel-aluminum layered double hydroxide as a nano-sorbent for the solid phase extraction of selenium, and its determination by continuous flow HG-AAS. Microchim. Acta 180, 619–626.
Alizadeh, M., Mehmandoust, M., Nodrat, O., et al., 2021. A glassy carbon electrode modified based on molybdenum disulfide for determination of folic acid in the real samples. J. Food Meas. Charact. 15, 5622–5629.
Amin, S., Tahira, A., Solangi, A., et al., 2019. A practical non-enzymatic urea sensor based on NiCo 2 O 4 nanoneedles. RSC Adv. 9, 14443–14451.
Ammeri, R.W., Mehri, I., Badi, S., et al., 2015. Pentachlorophenol degradation by Pseudomonas fluorescens. Water Qual. Res. J. 52, 99–108.
Auerbach, S.M., Carrado, K.A., Dutta, P.K., 2004. Handbook of Layered Materials. CRC Press.
Baig, N., Kawde, A.-N., 2015. A novel, fast and cost effective graphene-modified graphite pencil electrode for trace quantification of l-tyrosine. Anal. Methods 7, 9535–9541.
Baig, N., Kawde, A.-N., 2016. A cost-effective disposable graphene-modified electrode decorated with alternating layers of Au NPs for the simultaneous detection of dopamine and uric acid in human urine. RSC Adv. 6, 80756–80765.
Bukhtiyarova, M., 2019. A review on effect of synthesis conditions on the formation of layered double hydroxides. J. Solid State Chem. 269, 494–506.
dos Santos, M., Wrobel, E.C., dos Santos, V., et al., 2016. Development of an electrochemical sensor based on LbL films of Pt nanoparticles and humic acid. J. Electrochem. Soc. 163, B499.
Feng, S., Yang, R., Ding, X., et al., 2015. Sensitive electrochemical sensor for the determination of pentachlorophenol in fish meat based on ZnSe quantum dots decorated multiwall carbon nanotubes nanocomposite. Ionics 21, 3257–3266.
Jijoe, P.S., Yashas, S.R., Shivaraju, H.P., 2021. Fundamentals, synthesis, characterization and environmental applications of layered double hydroxides: a review. Environ. Chem. Lett. 19, 2643–2661.
Jiménez-López, B., Leyva-Ramos, R., Salazar-Rábago, J., et al., 2021. Adsorption of selenium (iv) oxoanions on calcined layered double hydroxides of Mg-Al-CO3 from aqueous solution. Effect of calcination and reconstruction of lamellar structure. Environ. Nanotechnol. Monit. Manage. 16, 100580.
Jin, W., Maduraiveeran, G., 2017. Electrochemical detection of chemical pollutants based on gold nanomaterials. Trends Environ. Anal. Chem. 14, 28–36.
Kang, Q., Yang, L., Chen, Y., et al., 2010. Photoelectrochemical detection of pentachlorophenol with a multiple hybrid CdSe x Te1− x/TiO2 nanotube structure-based label-free immunosensor. Anal. Chem. 82, 9749–9754.
Khand, N.H., Palabiyik, I.M., Buledi, J.A., et al., 2021. Functional Co 3 O 4 nanostructure-based electrochemical sensor for direct determination of ascorbic acid in pharmaceutical samples. J. Nanostruct. Chem. 1–14.
Kikhtyanin, O., Čapek, L., Tišler, Z., et al., 2018. Physico-chemical properties of MgGa mixed oxides and reconstructed layered double hydroxides and their performance in aldol condensation of furfural and acetone. Front. Chem. 6, 176.
Kumar, A.K.S., Zhang, Y., Li, D., et al., 2020. A mini-review: How reliable is the drop casting technique? Electrochem. Commun. 121, 106867.
Lee, C.-C., Guo, Y.L., Kuei, C.-H., et al., 2006. Human PCDD/PCDF levels near a pentachlorophenol contamination site in Tainan, Taiwan. Chemosphere. 65, 436–448. https://doi.org/10.1016/j.chemosphere.2006.01.063.
Liang, H., Li, L., Meng, F., et al., 2015. Porous two-dimensional nanosheets converted from layered double hydroxides and their applications in electrocatalytic water splitting. Chem. Mater. 27, 5702–5711.
Maduraiveeran, G., Jin, W., 2017. Nanomaterials based electrochemical sensor and biosensor platforms for environmental applications. Trends Environ. Anal. Chem. 13, 10–23.
Mallakpour, S., Radfar, Z., Hussain, C.M., 2021. Current advances on polymer-layered double hydroxides/metal oxides nanocomposites and bionanocomposites: Fabrications and applications in the textile industry and nanofibers. Appl. Clay Sci. 206, 106054.
Mehmandoust, M., Erk, N., Alizadeh, M., et al., 2021. Voltammetric carbon nanotubes based sensor for determination of tryptophan in the milk sample. J. Food Meas. Charact. 15, 5288–5295.
Meskher, H., Achi, F., Moussa, F.B., et al., 2023. A novel pentachlorophenol electrochemical sensor based on nickel-cobalt layered double hydroxide doped with reduced graphene oxide composite. ECS Adv. 2, 016503.
Mustafa, Y.F., 2023a. Coumarins from carcinogenic phenol: synthesis, characterization, in silico, biosafety, anticancer, antioxidant, and anti-inflammatory assessments. Chem. Pap. https://doi.org/10.1007/s11696-023-03105-7.
Mustafa, Y.F., 2023b. Modern developments in the application and function of metal/metal oxide nanocomposite-based antibacterial agents. BioNanoScience 13, 840–852. https://doi.org/10.1007/s12668-023-01100-6.
Remes, A., Pop, A., Manea, F., et al., 2012. Electrochemical determination of pentachlorophenol in water on a multi-wall carbon nanotubes-epoxy composite electrode. Sensors 12, 7033–7046.
Sajid, M., Nazal, M.K., Mansha, M., et al., 2016. Chemically modified electrodes for electrochemical detection of dopamine in the presence of uric acid and ascorbic acid: a review. TrAC Trends Anal. Chem. 76, 15–29.
Salmanpour, S., Abbasghorbani, M., Karimi, F., et al., 2017. Electrocatalytic determination of cysteamine uses a nanostructure based electrochemical sensor in pharmaceutical samples. Curr. Anal. Chem. 13, 40–45.
Saratale, R.G., Saratale, G.D., Shin, H.S., et al., 2018. New insights on the green synthesis of metallic nanoparticles using plant and waste biomaterials: current knowledge, their agricultural and environmental applications. Environ. Sci. Pollut. Res. 25, 10164–10183.
Taqvi, S.I.H., Solangi, A.R., Buledi, J.A., et al., 2022. Plant extract-based green fabrication of nickel ferrite (NiFe2O4) nanoparticles: an operative platform for non-enzymatic determination of pentachlorophenol. Chemosphere 294, 133760.
Tonelli, D., Scavetta, E., Giorgetti, M., 2013. Layered-double-hydroxide-modified electrodes: electroanalytical applications. Anal. Bioanal. Chem. 405, 603–614.
Wang, L., Li, X., Yang, R., et al., 2020. A highly sensitive and selective electrochemical sensor for pentachlorophenol based on reduced graphite oxide-silver nanocomposites. Food Anal. Methods 13, 2050–2058.
Wang, Q., O'Hare, D., 2012. Recent advances in the synthesis and application of layered double hydroxide (LDH) nanosheets. Chem. Rev. 112, 4124–4155.
Ya, Y., Jiang, C., Yan, F., et al., 2018. A novel electrochemical sensor for chlorophenols based on the enhancement effect of Al-doped mesoporous cellular foam. J. Electroanal. Chem. 808, 107–113.
Yang, M., Chen, Y., Wang, H., et al., 2022. Solvothermal preparation of CeO2 nanoparticles–graphene nanocomposites as an electrochemical sensor for sensitive detecting pentachlorophenol. Carbon Letters. 32, 1277–1285.

Yu, J., Wang, Q., O'Hare, D., et al., 2017. Preparation of two dimensional layered double hydroxide nanosheets and their applications. Chem. Soc. Rev. 46, 5950–5974.
Yuan, S., Peng, D., Hu, X., et al., 2013. Bifunctional sensor of pentachlorophenol and copper ions based on nanostructured hybrid films of humic acid and exfoliated layered double hydroxide via a facile layer-by-layer assembly. Anal. Chim. Acta 785, 34–42.
Zhang, W., G. Zhu, J. Ma, et al., 2011. A new electrochemical sensor based on W-doped titania-CNTs composite for detection of pentachlorophenol.
Zhang, Y., Xu, H., Lu, S., 2021. Preparation and application of layered double hydroxide nanosheets. RSC Adv. 11, 24254–24281.
Zhao, D., 2014. Determination of pentachlorophenol residue in meat and fish by gas chromatography–electron capture detection and gas chromatography–mass spectrometry with accelerated solvent extraction. J. Chromatogr. Sci. 52, 429–435.
Zhao, P., Li, N., Astruc, D., 2013. State of the art in gold nanoparticle synthesis. Coord. Chem. Rev. 257, 638–665.
Zhou, Y., Jiang, Q., Peng, Q., et al., 2007. Development of a solid phase microextraction-gas chromatography–mass spectrometry method for the determination of pentachlorophenol in human plasma using experimental design. Chemosphere 70, 256–262.